KES Transactions on Sustainable Design and Manufacturing I
Sustainable Design and Manufacturing 2014 : pp.936-949 : Paper sdm14-077

Investigations on repetition rate and laser wavelength for efficient generation of black silicon solar cells

Viktor Schütz, Jürgen Koch, Oliver Suttmann, Ludger Overmeyer

Laser Zentrum Hannover e.V., Hollerithallee 8, 30419 Hannover, Germany
v.schuetz@lzh.de

Abstract Ultra-short pulsed laser radiation applied on silicon decreases the reflectivity by modifying the surface topology by ablation to achieve a so called "black silicon" texture. A multitude of laser processing parameters are investigated in order to classify the reflectivity reduction. Exemplarily, 5-inch mc-silicon solar wafers are machined in a first step with high throughput using a linear 7-foci diffractive optical element (DOE). In a second step, solar cells are built up to determine the efficiency gain by the laser surface modification. A preliminary absolute efficiency gain of $\Delta\eta > 0.2\,\%$ is achieved at an absolute reflectivity reduction of globally 11.2 % in comparison to a conventional isotexture.
KEYWORDS: laser, surface modification, black silicon, solar cells, mc-silicon

1 Introduction

In photovoltaic applications, low spectrally independent reflectivity is desired, in order to achieve high absorption in the relevant solar spectral range, and result in high cell efficiency. However, silicon has a high spectral dependent reflectivity. Reflectivity can be reduced by surface structuring and applying antireflective coatings (ARC) [1]. A major disadvantage of an ARC is the small spectral range for reflectivity reduction in the order of a few tens of nm. The reflectivity of crystalline silicon can alternatively be reduced by laser surface modification of the topology. Surface features can be generated with a high symmetry or surface feature distributions at short and ultra-short laser radiation [2][3][4], as well as with non-radiative techniques [5]. A spectrally weighted reflectivity of approx. 8 % for textured silicon produced by etching can be achieved. Laser-induced groove structures on silicon reduce the reflectivity from 34 % to 28 % with an additional post processing by etching [3].
A cone-like texture is generated using SF_6 gas in combination with multiple nearinfrared (NIR) femtosecond laser radiation pulses [2][6][7], or ultraviolet (UV) radiation with a pulse duration of a few ns [4]. The absorption of a photon in silicon with an energy lower than the bandgap energy is improved using femtosecond laser processing with the additive gas SF_6. During laser processing, SF_6 is decomposed to fluorine and sulphur radicals [8][9]. Sulphur is a dopant for silicon, locally reducing the bandgap energy by having additional energetic levels between the valence and conduction band.

This absorption improvement at photon energies lower than the bandgap is not desirable for photovoltaic applications, because the electrons cannot transit from the valence into the conduction band, and therefore the increased absorption at larger wavelengths yield additional losses due to decay of phonons, resulting in increased heat input at smaller photon energies, and thereby lowering the efficiency of solar cells. Further, the decreased bandgap yields, even for ideal conversion, lower maximum solar cells efficiency according to the Queisser-Shockley limit [10].

While the fundamental formation of the cone-like structure is independent of any additive gases, some gases can change the structuring process [2][6][7]. Laser sources with a pulse duration in the femtosecond range with low repetition rates in the 1 kHz range, and therefore low area velocities (square meters per second) are used for the laser texturing process to generate cone-like structures. The formation mechanism of these cone-like structures is not yet understood in great detail, but some first empirical calculations on the growth process of these structures have been carried out [5], and basics of the formation of these cone-like structures and their dependencies on processing gases and laser process parameters have been investigated [2][6][7].

In our work, a laser based surface modification technique for mc-Si solar cells with a high processing velocity is presented. Our technique does not require additional chemical additives, and is carried out in ambient atmosphere. As SF_6 is not used, there is no need for complex gas recycling or safety engineering for dangerous materials, and setup, and the experimental results are compared to normal ambient atmosphere. In order to determine the proper laser and ambient parameters for reflection reduction, two laser wavelengths and different repetition rates are investigated for a distinct number of laser pulses per point at a constant pulse duration of $t_p \approx 7\ \mathrm{ps}$.

Processed cells are generated, and the reflectivity as well as photovoltaic parameters are determined to evaluate the efficiency increase of the processed multicrystalline silicon (mc-Si) solar cells in comparison to non-laser processed samples.

In chapter 2, the experimental setup is described as well as the diagnostics used for evaluation of the process data.

The experimental results are presented and discussed in chapter 3. In detail, the ablation rate as a function of laser fluence is determined. With respect to ablation, different achievable surface topologies are presented. At distinct laser fluences, structuring results are presented for the laser wavelengths $\lambda = 515\ \mathrm{nm}$ and $\lambda = 1030\ \mathrm{nm}$ at different repetition rates and for ambient gases. The structures are evaluated in terms of the structuring depth, topology and the normalized gray scale value (NGSV) of the surface darkness, which is a qualitative measure of the reflectivity. In order to determine the laser-induced surface damage, the minority carrier lifetime has been measured using µ-PCD on silicon float zone wafers.

Furthermore, the spectrally dependent reflectivity has been determined for a sample of completely processed 5-inch solar wafers, as well as the electrical properties of the finished solar cell.

2 Experimental Setup and Diagnostics

The laser structuring setup consists of an ultra-fast laser source with an optional second harmonic generator ($t_p \approx 7$ ps, $\lambda = 1030 / 515$ nm, $f_{rep} \leq 400$ kHz, $M^2 \approx 1.2$), a three times beam expander, and a scanner system, Figure 1. The scanner is equipped with a dichroitic f-theta objective with a focal length of 255 mm for $\lambda = 1030$ nm or $\lambda = 515$ nm. Laser spot diameters at the sample surface at 1/e² of $d_{foc,515nm} = 20$ µm and $d_{foc,1030nm} = 40$ µm have been measured using a Primes MicroSpotMonitor. Full 5-inch solar wafers have been processed using an additional diffractive optical element (DOE) for process parallelization [11].

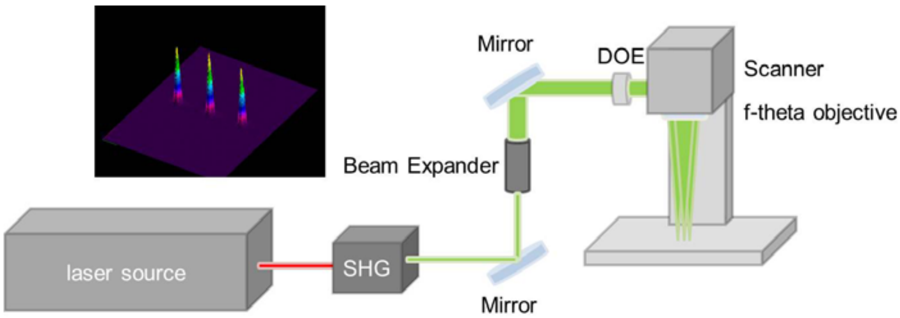

Figure 1: Experimental laser setup with optional DOE for process parallelization; measured intensity distribution

The $NGSV$ (normalized gray scale value) given as a measure of the reflectivity has been determined for constant orthogonal sample illumination. The data is collected using a color CCD-camera and converted to an 8-bit grayscale image with values from $NGSV = 1$ equalling white to $NGSV = 0$ equalling black. The distribution of the grayscale values in the laser treated area is averaged and the standard deviation of the $NGSV$ describes the deviation of the data due to e.g. different grain orientations. No physical or chemical post-processing of the laser treated area has been done.

Crystallographic defects induced by laser processing are studied for monocrystalline float zone silicon wafers with an initial minority carrier lifetime $\tau_{eff} > 900$ µs of the bulk. This investigation is carried out in order to evaluate the necessity of post processing to remove defects. After laser structuring, the samples are cleaned using standard RCA ($NH_4OH:H_2O_2:H_2O$ and $HCl:H_2O_2:H_2O$), and then passivated with a SiN-layer. The minority carrier lifetime is measured using microwave photoconductive decay (µ-PCD) method with a spatial resolution of

500 µm. The irradiated areas on the silicon are characterised with regard to their minority carrier lifetime by quantifying the average areal minority carrier lifetime.
Full 5-inch solar wafers have been processed applying a seven spot DOE for process parallelization [11]. In analogy to conventional solar cell processing in the photovoltaic industry, the wafers are etched, primarily to remove the saw damage and produce an isotexture. In this study, an additional laser texturing followed, and a damage removal step was added to the texturing process. Subsequent processing steps are not changed, see Figure 2.

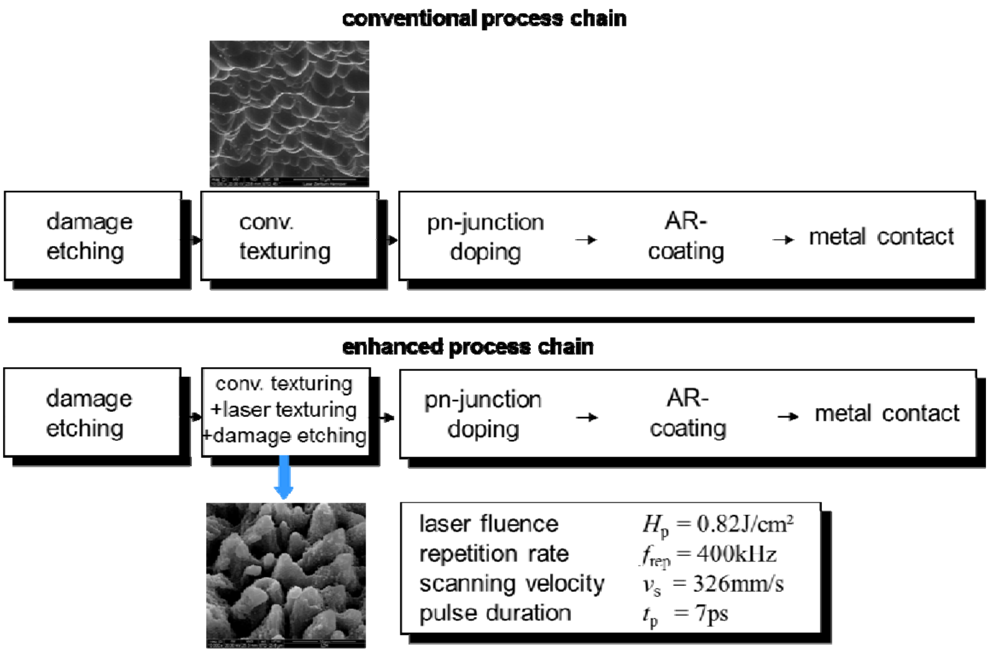

Figure 2: Modified processing chain for laser structuring to achieve a black silicon topology

3 Results and Discussion

3.1 Ablation studies and crystallographic results

The ablation of silicon using ultra-short laser radiation can be described by the two temperature model (TTM) [12][13]. Two ablation behaviors can be distinguished. For the optical penetration depth $\delta_{opt} >> \delta_{therm}$, ablation is given by shallow ablation grooves with “negligible” thermal damage of the material. Further, the penetration depth is given by optical absorption with large extinction coefficient of the laser radiation. However, multiple irradiations of the same area form a cone-like structure on the surface of silicon [2][6][7], and is expressed by the irradiation cycles during scanning with pulsed laser radiation with the geometry parameter

$$N_{\mathrm{ppp}} = \frac{d_{\mathrm{foc}} \cdot f_{\mathrm{rep}}}{\mathrm{v}} \tag{1}$$

with d_{foc} representing the focal spot diameter, f_{rep} the repetition rate, and v the scanning velocity. For the thermal penetration depth l, ablation is given by deep ablation grooves with definite thermal damage of the material. Further, in this case, the penetration depth l is determined by the thermal conductivity of the free electrons λ_{e-} of the laser treated material. Processing with large irradiation cycles N_{ppp} yield, in thermal ablation, deeper grooves, and in the optical ablation a cone-like structure, Figure 3.

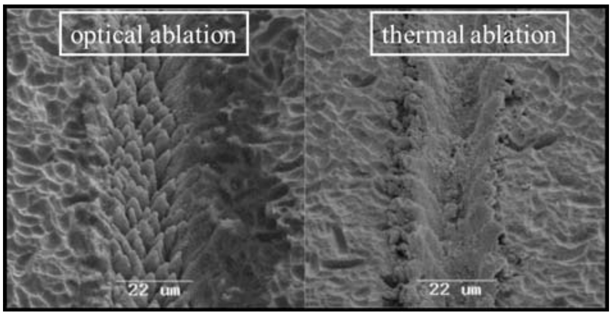

Figure 3: Exemplary topologies of laser ablated grooves; left: dense cone-like structures within the groove at H_p = 0.56 J/cm²; right: typical v-shaped ablated groove at H_p = 11.5 J/cm² [14]; ambient atmosphere at room temperature, no additive gases, λ = 515 nm, f_{rep} = 400 kHz, t_p ≈ 7 ps

The ablation threshold and the transition fluence is given in Figure 4a. A change in reflectivity has been visually detected for ablated structures at laser fluences above the ablation threshold, as well as the detected minority carrier lifetime τ_{eff}, which is a measure of crystal damage for silicon, which decreases significantly by two orders of magnitude without any dependence of repetition rate f_{rep} compared to its initial value, Figure 4b.

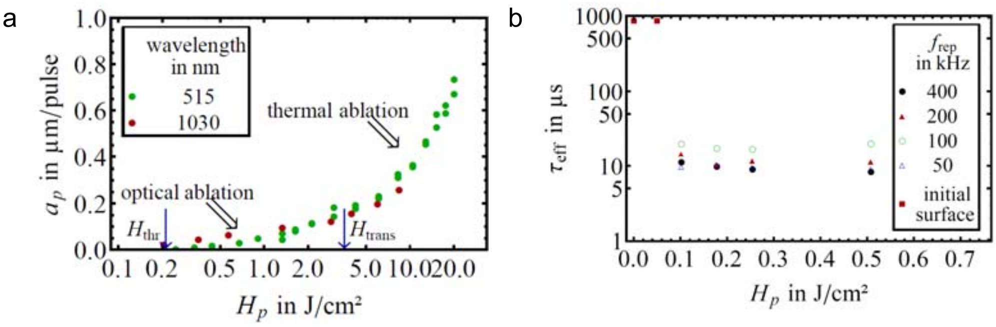

Figure 4: a) Ablation depth per pulse a_p versus laser fluence H_p for monocrystalline silicon <111> at a pulse duration of t_p = 7 ps; blue arrows show the ablation threshold and the transition fluence; b) Minority carrier lifetime τ_{eff} as a function of laser fluence H_p and repetition rate f_{rep} on monocrystalline silicon wafers obtained with µ-PCD, λ = 515 nm at N_{ppp} = 13.3

3.2 Laser structured surfaces

A parameter study has been carried out in order to determine suitable laser parameters for achieving a cone-like structure, different laser wavelengths λ, laser fluences H_p, repetition rates f_{rep}, number of pulses per point N_{ppp}, and ambient gases, see Table 1.

Table 1: Parameter regimes tested to achieve laser structuring of mc-Si

λ in nm	515	1030
H_p in J/cm²	0.1 – 10.0	
f_{rep} in kHz	1 - 400	
N_{ppp}	1 - 1000	
atmosphere	SF_6; O_2; ambient atmosphere	ambient atmosphere

The parametric field consisting of quadratic fields of 3x3 mm² has been processed at a laser fluence $H_p = 0.36$ J/cm², Figure 5. Each feature is laser treated with a specific f_{rep} and N_{ppp}.

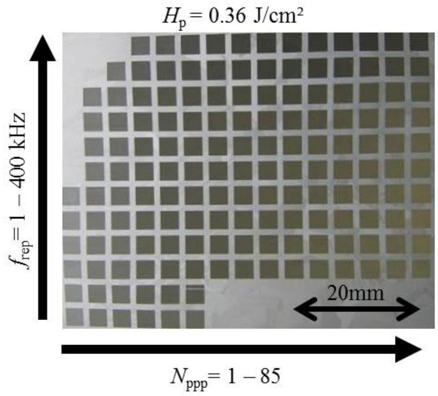

Figure 5: Parameter fields for λ = 1030 nm on a mc-Si wafer, detected by a CCD-camera; resolution: 1pixel = 45.5 μm x 45.5 μm

The laser structuring yields different degrees of darkened surface at different N_{ppp} and f_{rep}. The measure $NGSV$ is set one for white and zero for black for constant orthogonal sample illumination. A light gray surface is obtainable for low repetition rates and number of pulses per point, with e.g. $NGSV \approx 0.55$. At large f_{rep} and N_{ppp}, dark black areas are distinguished, with e.g. $NGSV \approx 0.25$. The lower the repetition rate, the more yellowish the coloration of the surface gets. The lowest $NGSV$ is determined for $f_{rep} = 400$ kHz at $N_{ppp} = 90$. Furthermore, $NGSV$ decreases with larger f_{rep} and N_{ppp} at $H_p = 0.36$ J/cm², Figure 6a. Additionally, higher laser fluences are investigated with respect to the evolution of $NGSV$ and N_{ppp} up to 1000 at a constant repetition rate $f_{rep} = 400$ kHz, Figure 6b. At $f_{rep} = 400$ kHz and $\lambda = 1030$ nm, similar low $NGSV$ is achieved for all investigated laser fluences. The higher the laser fluence, the less pulses are required to achieve the minimum of $NGSV$. The v-shaped grooves are observed at larger laser fluences in the thermal ablation regime, similar to Figure 3 right. At low fluences, e.g. $H_p = 0.56$ J/cm² cone-like structures are observed, similar to Figure 3 left.

The parameter fields are evaluated for $\lambda = 515$ nm in analogy to the wavelength $\lambda = 1030$ nm. The repetition rate $f_{rep} = 400$ kHz is first investigated with different fluences, Figure 6d. The distribution exhibits at all investigated fluences a local minimum around $N_{ppp} = 30\text{-}100$. For $H_p \leq 1.41$ J/cm² cone-like structures, for $H_p = 5.34$ J/cm² v-shaped grooves have been observed. The minimal $NGSV$ is measured for $H_p = 0.82$ J/cm² at $N_{ppp} \approx 50\text{-}60$. A similar low $NGSV$ at the minimum is also reached at $H_p = 5.34$ J/cm², but with a different topology. For the two other fluences, higher $NGSV$s are measured at the minimum, Figure 6d. Further, the repetition rate is altered at $H_p = 0.82$ J/cm², Figure 6c. Laser processing with N_{ppp} above 100 has not been investigated, due to oxidization of the surface. In contrast to $\lambda = 1030$ nm, no repetition rate dependent decrease of $NGSV$ has been distinguished.

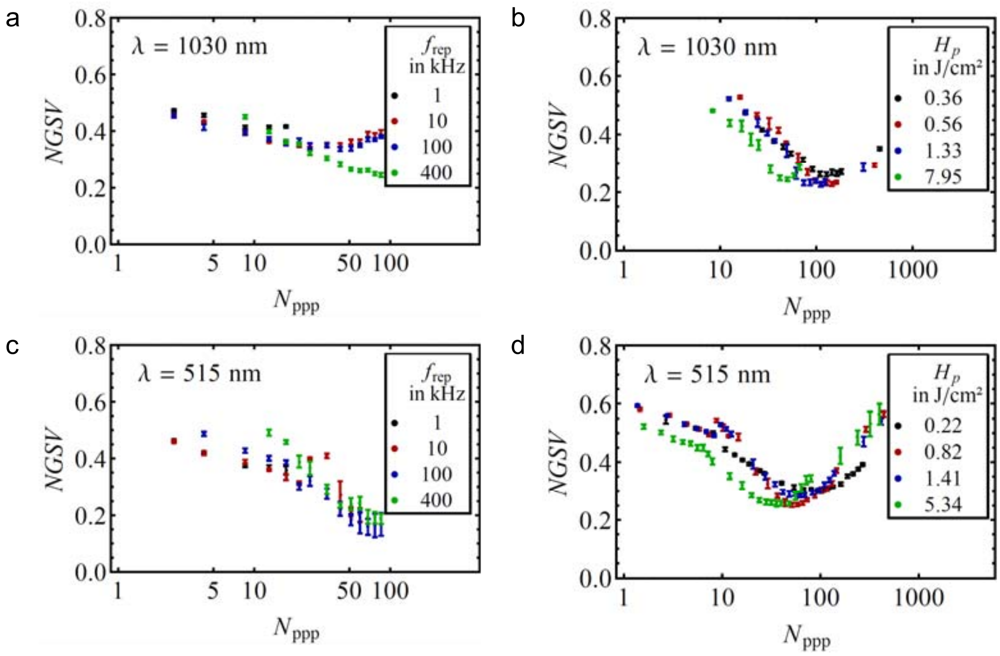

Figure 6: NGSV as a function of N_{ppp} of a mc – silicon wafer; a) H_p = 0.36 J/cm²; b) f_{rep} = 400 kHz; c) H_p = 0.82 J/cm²; d) f_{rep} = 400 kHz

3.3 Comparison of different ambient gases

The normal ambient gas atmosphere (78% N2, 21% O_2, 1% rest), nearly pure oxygen (O_2) and sulphur hexafluoride gas atmosphere (SF_6) are investigated, since they can decrease $NGSV$ at the laser wavelength $\lambda = 515$ nm. In agreement with other publications, the lowest reflectivity can be achieved with the gas SF_6 at large N_{ppp} [7], Figure 7a and Figure 7b.

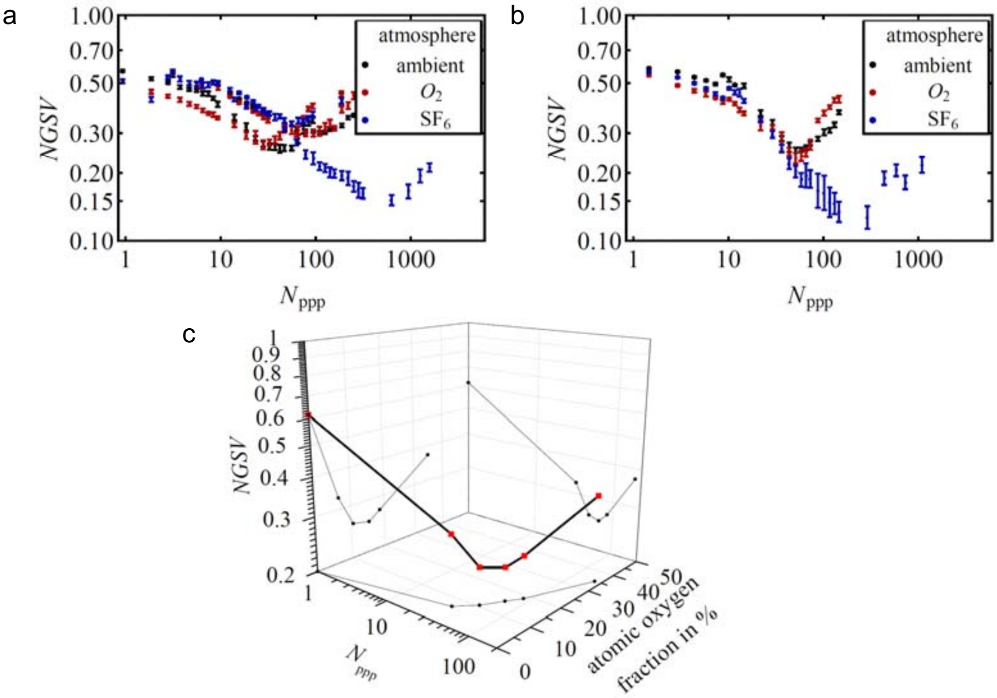

Figure 7: NGSV as a function of process gas; a) mc-Si wafer, λ = 515 nm, f_{rep} = 400 kHz, at different laser fluences, H_p = 0.26 J/cm² bottom and H_p = 5.34 J/cm² top curve; b) mc-Si wafer, λ = 515 nm, f_{rep} = 400 kHz, H_p = 0.82 J/cm²; c) NGSV as a function of atomic oxygen fraction in the laser processing width and N_{ppp}, mc-Si wafer, λ = 515 nm, f_{rep} = 400 kHz, H_p = 0.82 J/cm², projection of the curve to each dimensional plane to demonstrate the single interdependencies

For the nearly pure oxygen atmosphere as well as for the ambient atmosphere, minimal NGSV is achieved at $N_{\mathrm{ppp}} \approx 40\text{-}80$. A further decrease to $NGSV \approx 0.15$ is achieved in an SF_6 atmosphere and $N_{\mathrm{ppp}} \approx 200\text{-}300$. Different minimal $NGSVs$ are achievable, due to the different gaseous conditions and the remaining oxygen concentration in the processing atmosphere. No significant difference is obtainable for the different atmospheres up to $N_{\mathrm{ppp}} \approx 50$ at the fluence $H_{\mathrm{p}} = 0.82$ J/cm². For larger oxygen concentrations in the process atmosphere, lower NGSV are achievable, up to $N_{\mathrm{ppp}} \approx 50$ than using SF_6 gas. For larger N_{ppp} the gas SF_6 with a lower oxygen concentration in the processing atmosphere yields smaller values because of lower oxidization, Figure 7b. The atomic oxygen fraction in the laser processing area increases with N_{ppp} at fixed laser parameters. At the laser parameters mentioned in Figure 7c the minimum of $NGSV$ is reached at an atomic oxygen fraction of 15 % which is close to normal ambient atmosphere with 21 % oxygen. Further, oxidization yields an increase of $NGSV$, Figure 7c.

3.4 Large area processing of solar cells

The lowest reflectivity has been determined after laser processing with the gas SF_6, Figure 7a and Figure 7b. However, yellowish fine filaments have been observed irradiating at $\lambda = 515$ nm with a repetition rate of $f_{rep} = 400$ kHz during laser processing in SF_6 gas, Figure 8a. The filaments can be removed easily if they stick to the surface after laser processing, by applying compressed air. Ambient atmosphere is chosen for processing full wafers, Figure 8b. In an ambient atmosphere, the silicon surface is even more oxidized during laser processing, compared to SF_6 atmosphere. However, large-scale working with SF_6 needs a more complex experimental setup, due to gas scrubbing of SF_6. Further, the process is unstable, due to an excessive generation of fine filaments, which deflect laser radiation. Laser texturing is performed with the process parameters $N_{ppp} = 29$, $H_p = 0.82$ J/cm², with a seven spot diffractive element for process parallelization and normal ambient atmosphere, to minimize the processing time and to assure low $NGSV$. As a result, an area velocity of $v_a = 18.6$ mm²/s was achieved. After laser processing, no isotexture features of the original surface could be detected. The surface is completely transformed to a cone-featured surface topology. The decrease of the spectral dependent reflectivity in comparison to a single isotexture is presented for the same parameter set as in Figure 8c.
The mean reflectivity reduction in the range $300\ \text{nm} \leq \lambda \leq 1121\ \text{nm}$ with an additional laser texturing in comparison to the standard isotexture is approx. 11 %, Figure 8c. Adding an anti-reflective coating (SiN_x) to the isotexture and the lasertexture, the average reflectivity reduction equals $\Delta R = (4.02 \pm 0.02)$ %. As a result, the total efficiency gain determined for an average of five wafers is $\Delta\eta = 0.21$ %, respectively the relative gain is $\Delta\eta_{rel} = 1.34$ % compared to processed solar cells without additional laser texturing, with the above mentioned laser parameters. The efficiency gain is primarily due to the larger short circuit current J_{sc} because of the lower reflectivity R. The scattering of the reflectivity data yield a small variance in the short circuit current as well as the efficiency of the solar cells, Table 2.
With the currently available laser systems (average laser powers of ultra-short pulse laser radiation $P_{av} = 50\text{-}400$ W) cost-effective industrial production is not possible, due to high processing times. Processing times can be reduced with higher average laser powers in the kW range, and high-throughput process parallelization with diffractive optical elements (DOEs) [11].

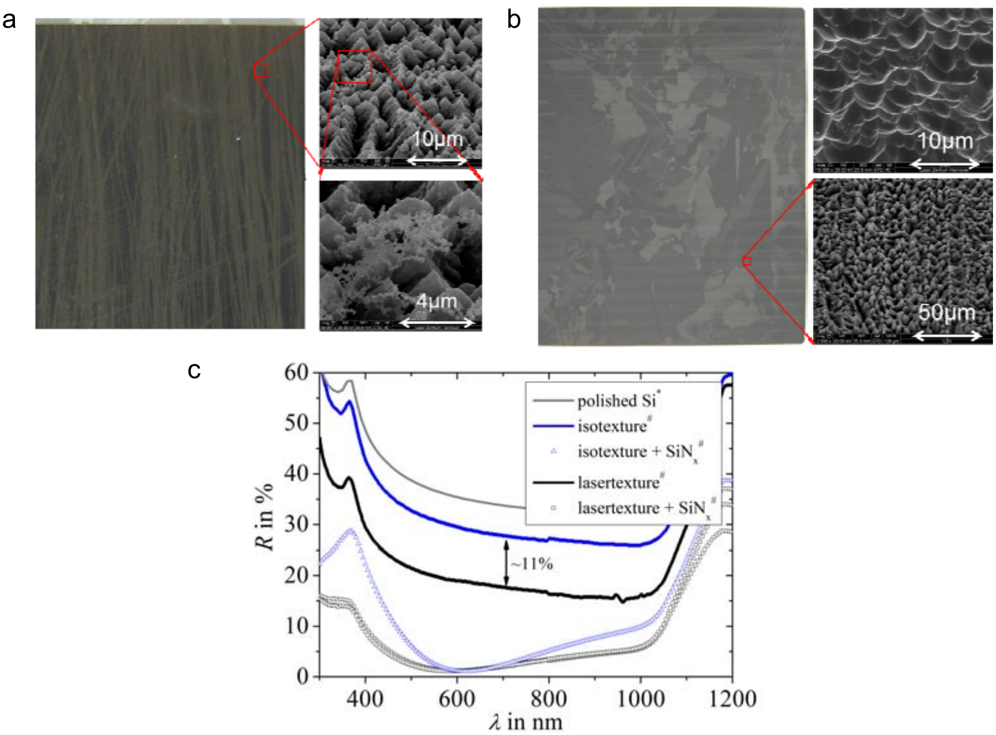

*Figure 8: Structured surface on a bare mc-Si wafer a) process atmosphere SF_6, λ = 515 nm, f_{rep} = 400 kHz, N_{ppp} = 34 and H_p = 0.36 J/cm²; filaments of sulphur can be seen on top of the black surface; b) Left: part of a full 5-inch mc-Si wafer textured with a seven spot diffractive element (H_p = 0.82 J/cm², f_{rep} = 400 kHz, N_{ppp} = 29, v_a = 18.6 mm²/s); right: comparison between iso textured (top) surface and additional laser textured surface (bottom); c) Wavelength dependent reflectivity R of an isotextured and additional laser textured mc-Si wafer; H_p = 0.82 J/cm², f_{rep} = 400 kHz, N_{ppp} = 29; * [15]; # data from Schott Solar AG*

Table 2: Mean values of a set of five solar cells due to an additional laser texturing, V_{oc} open-circuit voltage, J_{sc} short-circuit current density, FF fill factor, η absolute efficiency, J_{rev} reverse current density; measured by Schott Solar AG

description	V_{oc} in mV	J_{sc} in mA/cm²	FF in %	η in %	J_{rev} in mA/cm²
isotexture	608.0 ± 1.1	34.10 ± 0.12	75.78 ± 0.32	15.71 ± 0.09	7.99 ± 2.10
isotexture+laser texturing+damage etching	604.6 ± 1.1	34.76 ± 0.13	75.78 ± 0.50	15,92 ± 0.09	8.57 ± 0.88
difference	-3.4	0.66	0	**0.21**	0.57

4 Conclusion

Laser-induced ablation of silicon yields different topologies with respect to the laser parameters used. Applying laser radiation close to H_{th} in the optical ablation regime, and multiple irradiation cycles yields a cone-shaped topology. Using fluences above $>> H_{\mathrm{th}}$ yields typical v-shaped laser grooves. Both topologies reduce reflectivity if structure height is larger than wavelength, due to multiple reflections at the interfaces of the cones or grooves. In general, the reflectivity for structured surfaces is a function of the structure height Θ, and the periodicity Λ. For a structure height Θ, a simple boundary consideration can be distinguished, due to the light wavelength used, see Table 3.

Table 3: Boundary consideration for the interaction of light with structured surfaces

Mechanism	Relation
Diffraction	$\lambda >> \Theta$
Diffraction and Reflection	$\lambda \approx \Theta$
Reflection	$\lambda << \Theta$

For optical penetration depth and laser fluences up to several J/cm² and multiple irradiation cycles, cone-like structures are achievable. The overall reflectivity can be described as a function of structure height and periodicity, if the structure height is much larger than the wavelength of the incident light. Simple ray tracing is applicable, and the overall reflectivity is a function of multiple reflections [1][16]. In the other cases, diffraction has to be considered. The shape of the cone feature as well as their size depends strictly on the laser parameters. Linear scaling of process parameters yields similar but not identical topologies. Thus, the cone topology as a result of laser processing is a function of the laser fluence, laser wavelength, number of pulses per point and repetition rate.

Significant crystallographic damage has been detected for all laser parameter sets at multiple irradiation cycles. The silicon crystal is immediately damaged for laser fluences above H_{th}. In fact, in all cases, the laser induced damage has to be removed in order to avoid recombination at the silicon surface for efficient solar cells.

Two different laser wavelengths have been studied, in order to produce a cone-structured topology. The local heating due to laser radiation varies for $\lambda = 1030\ \mathrm{nm}$ and $\lambda = 515\ \mathrm{nm}$, with respect to their different optical penetration depths. Laser radiation at a wavelength of $\lambda = 1030\ \mathrm{nm}$ is absorbed by the silicon over a large volume, and for $\lambda = 515\ \mathrm{nm}$ close to the surface at approx. 1 µm at an ambient temperature of 300 K. The optical penetration length is also a function of temperature, with larger optical penetration depths at lower temperatures, and smaller optical penetration depths for higher temperatures. In conclusion, the absorbance behavior of silicon changes in the near infrared wavelength spectrum, from a volume to a surface characteristic [17]. The minimal temperature of the material surrounding the laser processing area rises with multiple irradiation cycles for short pulse time delays, respectively high repetition rates and laser fluence. In conclusion, the ablation rate increases with higher repetition rates and therefore lower $NGSV$ are achievable at $f_{\text{rep}} = 400\ \text{kHz}$, compared to 10 kHz. For $\lambda = 515\ \text{nm}$, no repetition rate dependence of $NGSV$ has been observed, but lower $NGSV$ in comparison to $\lambda = 1030\ \text{nm}$ have been found. The optical penetration depth of $\lambda = 515\ \text{nm}$ decreases from approx. 1 µm to several tens of nm at higher surface temperatures, which corresponds to the optical penetration depth determined with the two-temperature model. This percentile decrease is much smaller than for near infrared laser radiation. Therefore, this repetition rate dependence is not observed, respectively not observed for the laser parameters used. The increase of NGSV at $f_{\text{rep}} = 400\ \text{kHz}$ in comparison to e.g. $f_{\text{rep}} = 133\ \text{kHz}$ can be explained by a higher heat load, due to laser processing. In conclusion an optimized repetition rate for processing can be determined for each laser wavelength and laser fluence.

For laser radiation at $\lambda = 515\ \text{nm}$, different gaseous media are investigated, namely normal ambient atmosphere (78% N2, 21% O_2, 1% rest), nearly pure oxygen atmosphere (O_2) and sulphur hexafluoride gas (SF_6). The decrease of NGSV as a function of N_{ppp} is similar for all gaseous media up to $N_{\text{ppp}} \approx 50$. For larger N_{ppp}, processing with SF_6 yields the lowest $NGSV$. At larger N_{ppp}, porous SiO_2 is formed on the surface and superposes the cone featured texture. Higher laser fluences and oxygen concentration in the atmosphere used intensifies oxidization on the surface. However, the normal ambient atmosphere is a good compromise between processing with SF_6, which achieves lower $NGSV$ at larger N_{ppp}, and oxygen atmosphere, in which silicon is highly oxidized at lower N_{ppp}.

Processing of a large area at a high repetition rate in normal ambient atmosphere, and atmosphere containing SF_6 differs greatly. For the SF_6 atmosphere, loose sulphur particles arranged in fine filaments are generated, while for the ambient atmosphere, small bounded oxidized particles or layers are formed on the surface of silicon. The loose sulphur particles arranged in fine filaments can release of the surface and hinder the laser surface processing. Stable processing is not possible. A robust processing in normal ambient atmosphere with additional beam sampling for process parallelization on a large scale surface contrary to SF_6 gas has been achieved.

A preprocessing to achieve an isotexture surface topology is not required anymore, because the surface is completely geometrically reorganized with a cone topology. The cone feature sizes can be adjusted to a multiple of ratios of height and width. Under certain conditions of height and width, less surface reflectivity can be achieved with laser texturing. An 11 % lower reflectivity has been achieved in comparison to isotexture with and without an additional anti-reflective coating (SiN_x). Therefore, additional charge carriers (short-circuit current density $\Delta J_{\text{sc}} = +0.66\ \text{mA/cm}^2$) are generated, due to more absorbed light. As a consequence, a higher solar cell efficiency with an absolute efficiency gain of $\Delta\eta = 0.21\ \%$ is measured. The efficiency gain is primarily due to an increased short-circuit current density at a slightly smaller open-circuit voltage and the same fill factor.

5 Summary and Outlook

Laser processing of silicon to produce a cone-featured surface topology, also called "Black Silicon" is established. An efficiency gain for silicon solar cells has been achieved. The investigated laser wavelengths can be used for processing, but at different repetition rates, due to different applied heat loads as a reason of the optical penetration depth. Further, normal ambient atmosphere is suitable, as oxidization of the surface does not hinder the texturing process up to the number of pulses per point $N_{ppp} \approx 60$. A significant reflectivity reduction, and therefore an efficiency gain of a silicon solar cell based on laser processing in ambient atmosphere can be achieved at $20 < N_{ppp} < 60$. There is no benefit of using the gas SF_6 for laser texturing up tp $N_{ppp} = 60\text{-}70$. Texturing with larger N_{ppp} requires a higher processing time. A further reflectivity reduction is only achievable at lower oxygen concentrations in the processing atmosphere and larger N_{ppp}. A very low reflectivity can be achieved with SF_6 gas at $N_{ppp} \geq 80$.
Furthermore, larger area velocities can be achieved using commercially available picosecond lasers. With a laser output power of 400 W, a maximum area velocity of $v_a = 920\ \mathrm{mm^2/s}$ could be achieved [11]. An efficiency gain of $\Delta\eta = 0.21\ \%$ at an area velocity of $v_a = 18.6\ \mathrm{mm^2/s}$ has been presented. In future, mechanisms will be investigated to avoid excessive oxidization of the silicon surface during laser processing, but still using ambient atmosphere. Further, studies must be done on whether the raw, sawed wafers can also be used for laser surface processing with only one damage removal etch to reduce processing steps for silicon solar cell production.

Acknowledgement

We would like to thank Dr. H. Nagel from Schott Solar AG for fabrication and evaluation of the laser processed silicon wafers to solar cells. We would also like to thank our former colleague Prof. Dr. A. Horn for fruitful discussions and comments on this topic.

References

[1] Ekai, R., Verbeek, M., Nagel, H.: Optimisation of SiN antireflection coatings for encapsulated and non-encapsulated silicon solar cells with V-groove surface texture, In *Proc. 2nd World Conference on Photovoltaic Solar Energy Conversion*, pp.1430-1433, Austria, Vienna (1998)

[2] Tull, B.R., Carey, J.E., Mazur, E.: Silicon surface morphologies after femtosecond laser irradiation, In *MRS Bulletin*, vol. 31, pp. 626-633 (2006)

[3] Dobrzański, L.A., and Drygała, A.: Surface texturing of multicrystalline silicon solar cells, In *Journal of Achievements in Materials and Manufacturing Engineering*, vol. 31-1, pp. 77-82 (2008)

[4] Dehghanpour, H.R., Parvin, P., Sajad, B., and Nour-Azar, S.S.: Dose and pressure dependence of silicon microstructure in SF_6 gas due to excimer laser irradiation, In *Applied Surface Science*, vol. 255; pp. 4664-4669 (2009)

[5] Koynov, S., Brandt, M.S., and Stutzmann, M.: Black multi-crystalline silicon solar cells, In *Physica Status Solidi RRL*, Wiley: Weinheim, pp. 53-55; DOI: 10.1002/pssr.200600064 (2007)

[6] Carey, J.E. III.: Femtosecond-laser Microstructuring of Silicon for Novel Optoelectronic Devices, *PhD-Thesis*, Harvard University Cambridge (2004)

[7] Tull, B.R.: Femtosecond Laser Ablation of Silicon: Nanoparticles, Doping and Photovoltaics, *PhD-Thesis*, Harvard University Cambridge (2007)

[8] Stone, J., and Goodman, M.F.: Laser-induced multiphoton decomposition: isotope separation in SF_6, In *Chemical Physics Letters*, vol. 44-3, pp. 411-414, DOI: 10.1016/0009-2614(76)80694-X (1976)

[9] Dehghanpour, H.R., and Parvin, P.: Excimer and Nd:YAG laser-induced SF_6 decomposition at the vicinity of amorphous SiO_2 glas, *Applied Physics B: Lasers and Optics*, 101, 611-616, DOI: 10.1007/s00340-010-4141-4 (2010)

[10] Shockley, W., and Queisser, H.J.: Detailed Balance Limit of Efficiency of p-n Junction Solar Cells, In *Journal of Applied Physics*, vol. 32; pp. 510; DOI: 10.1063/1.1736034 (1961)

[11] Schütz, V., Horn, A., and Stute, U.: High-throughput process parallelization for laser surface modification on Si-Solar cells: determination of the process window, In *Proc. SPIE Vol. 8244-33*, USA, San Francisco (2012)

[12] Chichkov, B.N: Femtosecond, picosecond and nanosecond laser ablation of solids, In *Journal of Applied Physics A*, vol. 63, pp. 109-115 (1996)

[13] Dausinger, F., Hügel, H., Konov, V., Micro-machining with ultrashort laser pulses: From basic understanding to technical applications, In *Advanced Laser Technologies*, Adelboden, Switzerland (2002)

[14] Haupt, O., Schütz, V., Kling, R.: Improved laser edge isolation of crystalline silicon solar cells using a high power picosecond laser, In *Proc. 28th ICALEO*, M903, USA, Orlando (2009)

[15] Green, M.A. and Keevers, M.: Optical properties of intrinsic silicon at 300 K, In *Progress in Photovoltaics*, vol. 3, pp. 189-192 (1995)

[16] Sarnet, T., Halbwax, M., Torres R.: Femtosecond laser for black silicon and photovoltaic cells, In *Proc. of SPIE Vol. 6881 688119-1*, USA, San Jose (2008)

[17] Haupt, O.: Abtragsfreies Trennen von kristallinem Silizium mit kontinuierlicher Laserstrahlung, *PhD-Thesis*, University of Hannover (2009)